DESIGN OF NON-ISOLATED DC-DC CONVERTER FOR PHOTOVOLTAIC APPLICATION

DISSERTATION/THESIS

SUBMITTED IN PARTIAL FULFILLMENT OF THE REQUIREMENTS
FOR THE AWARD OF THE DEGREE
OF
MASTER OF TECHNOLOGY
IN
POWER ELECTRONICS & SYSTEMS

Submitted by:
UMA SHANKAR SONI
2K24/PES/07
Under the supervision of
DR. VANJARI VENKATA RAMANA
(Assistant Professor, EED, DTU)

DEPARTMENT OF ELECTRICAL ENGINEERING
DELHI TECHNOLOGICAL UNIVERSITY
(Formerly Delhi College of Engineering)
Bawana Road, Delhi-110042

MAY, 2026

M.Tech(Power Electronics and Systems) **UMA SHANKAR SONI** **2026**

DEPARTMENT OF ELECTRICAL ENGINEERING

DELHI TECHNOLOGICAL UNIVERSITY

(Formerly Delhi College of Engineering)

Bawana Road, Delhi-110042

CANDIDATE'S DECLARATION

I, **UMA SHANKAR SONI**, Roll No. 2K24/PES/07 student of M. Tech (Power Electronics & Systems), hereby declare that the project Dissertation titled **"Design of Non-Isolated DCDC Converter for Photovoltaic Applications"** which is submitted by me to the Department of Electrical Engineering Department, Delhi Technological University, Delhi in partial fulfillment of the requirement for the award of the degree of Master of Technology, is original and not copied from any source without proper citation. This work has not previously submitted for the award of any Degree, Diploma.

Place: Delhi **(Uma Shankar Soni)**

Date: 30/05/2026

DEPARTMENT OF ELECTRICAL ENGINEERING
DELHI TECHNOLOGICAL UNIVERSITY
(Formerly Delhi College of Engineering)
Bawana Road, Delhi-110042

CERTIFICATE

I hereby certify that the project Dissertation titled **"Design of Non-Isolated DC-DC Converter for Photovoltaic Applications"** which is submitted by Uma Shankar Soni, Roll No. 2K24/PES/07, Department of Electrical Engineering, Delhi Technological University, Delhi in partial fulfilment of the requirement for the award of the degree of Master of Technology, is a record of the project work carried out by the student under my supervision. To the best of my knowledge this work has not been submitted in part or full for any Degree or Diploma to this University or elsewhere.

Place: Delhi **DR. VANJARI VENKATA RAMANA**

Date: 30.05.2026 **(SUPERVISOR)**

DEPARTMENT OF ELECTRICAL ENGINEERING
DELHI TECHNOLOGICAL UNIVERSITY
(Formerly Delhi College of Engineering)
Bawana Road, Delhi-110042

ACKNOWLEDGEMENT

I would like to express my gratitude towards all the people who have contributed their precious time and effort to help me without whom it would not have been possible for me to understand and complete the project.

I would like to thank **Dr. Vanjari Venkata Ramana** (Assistant Professor, Department of Electrical Engineering, DTU, Delhi) my Project guide, for supporting, motivating and encouraging me throughout the period of this work was carried out. His readiness for consultation at all times, his educative comments, his concern and assistance even with practical things have been invaluable. I would also like to thank the Centre of Excellence for Electric Vehicles and Related Technologies, Delhi Technological University for providing necessary facilities for performing my research work.

Finally, I must express my very profound gratitude to my parents, seniors and to my friends for providing me with unfailing support and continuous encouragement throughout the research work.

Date: 30/05/2026

Uma Shankar Soni
M.Tech (Power Electronics & Systems)
Roll No. 2K24/PES/07

ABSTRACT

The increasing integration of photovoltaic (PV) systems into modern power networks requires efficient power conversion to overcome the inherent variability of solar energy. This paper presents the design and analysis of a DC–DC power converter for photovoltaic applications, aimed at maximizing energy extraction and ensuring regulated power delivery to the load or grid. A suitable converter topology is optimized to match the PV module characteristics, and Maximum Power Point Tracking (MPPT) algorithms are implemented to enhance system efficiency under varying irradiance and temperature conditions.

This thesis presents the design and analysis of a quadratic boost converter (QBC) for photovoltaic applications. The quadratic boost converter provides higher voltage gain compared to conventional boost converters without requiring extreme duty cycles. The proposed converter consists of two inductors, two capacitors, a diode network, and a controlled switching device to achieve quadratic voltage amplification. The converter is designed to improve voltage gain, reduce switching stress, and increase efficiency in solar energy systems. A maximum power point tracking (MPPT) technique is incorporated to extract maximum power from the PV module under varying environmental conditions. MATLAB/Simulink simulations are used to evaluate the performance of the proposed converter.

Simulation results shows that the quadratic boost converter effectively increases the output voltage and improves system efficiency while maintaining stable operation. The proposed system is suitable for renewable energy applications such as DC microgrids, battery charging systems, and solar-powered electronic devices.

TABLE OF CONTENTS

LIST OF FIGURES

LIST OF TABLES

LIST OF ABBREVIATIONS

EV	Electric Vehicle
QBC	Quadratic Boost Converter
PV	Photovoltaic
p.f.	Power Factor
THD	Total Harmonic Distortion
EMI	Electro Magnetic Interference
CCM	Continuous Current Mode
DCM	Discontinuous Current Mode
CC	Constant Current
CV	Constant Voltage
PFM	Pulse Frequency Modulation
PWM	Pulse Width Modulation
MPPT	Maximum Power Point Tracking
P&O	Perturb and Observe
DCR	Direct Current Resistance
ESR	Equivalent Series Resistance

LIST OF SYMBOLS

D	Duty Cycle
V_S	Input Voltage
D1, D2, D3	Diode
L1, L2	Inductor
C1, C2	Capacitor
S	Switch
R_L	Load Resistance
V0	O/P Voltage
f_s	Switching Frequency
Qc1, Qc2	Charge through capacitor C1 and C2
LTI	Linear Time-Invariant
PCB	Printed Circuit Board
Ir	Irradiance

CHAPTER 1

INTRODUCTION

1.1 Overview

Sustainable energy solutions are really essential in present scenarios. Renewable Energy sources like photovoltaic modules , do not produce the required voltage suitable for practical applications. To increase the voltage to required level, boost Converters are usually used. Boost Converters are not perfect. They can get hot and waste energy. Sometimes they even break [1].

The boost converter is one of the most common types of DC to DC converters employed for PV cells, owing to the simplicity of design, lower cost, and better control. Nevertheless, when a very high voltage gain is needed, there are many drawbacks associated with the conventional boost converter.

In case of the conventional boost converter, the voltage conversion ratio depends on the duty cycle. To obtain higher output voltage, a very high duty cycle operation should be employed by the converter. However, with increase in the duty cycle and approaching it to unity, there are a number of practical considerations. For example, higher conduction losses occur due to increased ON-state period of power switch. Moreover, there would be higher reverse recovery losses of the diode, and consequently switching losses will increase. Also, input current ripple and EMI levels would become higher with increasing duty cycle [1], [2].

Moreover, in this case, semiconductor devices experience high voltage stress due to higher voltage and current stress that occur in these cases. This requires employment of higher rated components, and hence higher costs. In addition, efficiency of such a converter is lowered due to higher conduction and switching losses. This becomes especially important in photovoltaic application due to lower input voltage and high DC-link voltage requirement. In addition, the traditional boost converter exhibits inferior dynamic response to rapidly varying environmental variables such as varying solar radiations and temperature. In addition, operation at high duty cycles may also result in stability problems and lower reliability of the DC-DC converters [2], [3].

The increasing popularity of renewable energy systems, electric cars, fuel cells, and microgrids has made high-gain DC–DC converters an increasingly important design goal. The typical output voltage of a PV module in a photovoltaic system ranges from 20 to 50 volts, while applications including grid-connected inverters, DC microgrids, and battery energy storage systems typically have requirements from 200 V to 400 V or more. Conventional converters such as the boost converter cannot perform such a significant voltage transformation efficiently [3], [5].

High-gain converters circumvent these issues through the use of strategies like coupled inductors, switched capacitors, voltage multiplier cells, quadratic structures, and interleaving. High-gain converters offer many advantages, among which is that they are capable of obtaining a high voltage gain without using high duty cycles, which helps reduce switching losses and improves efficiency [3], [4].

Among the available high-gain topologies, the quadratic boost converter has attracted considerable attention because it offers a significantly higher voltage gain than the conventional boost converter while maintaining a relatively simple structure and continuous input current. This makes it particularly suitable for photovoltaic applications where efficient energy extraction and voltage boosting are essential [4], [5].

Because photovoltaic systems can produce power from solar energy in an environmentally beneficial way, they have gained popularity. A photovoltaic panel's voltage is quite low and is dependent on temperature changes and sun radiation. A high-gain dc/dc converter is required to increase the output voltage from the photovoltaic cell to the necessary value because the low voltage obtained is insufficient for direct application, particularly for grid-connected systems, electric vehicles, battery charger units, and dc microgrids [1].

In solar systems, conventional boost converters are typically used as voltage boosters. A very high duty cycle is required when utilizing a typical boost converter in order to get a high voltage conversion ratio. Increased switching loss, voltage strains on semiconductor devices, and even conduction will result from such high duty cycle operation, lowering overall efficiency [2]. High gain converters, such as quadratic boost converters, are required to prevent these issues.

Additionally important for improving MPPT (Maximum Power Point Tracking) effectiveness is a high gain converter. To extract the most electricity from the solar panels, MPPT techniques must be used because the output characteristics of PV modules vary depending on the atmosphere. Stable functioning and improved power transfer efficiency are made possible by the use of a high gain converter [4].

Another benefit of using the converter in question is that it can reduce the size and complexity of the system. The reason for this is that high gain converters can convert large voltage ratios without requiring large transformers. Consequently, the system will become compact and economical. Furthermore, it is well known that the majority of high gain converters are continuous input current converters [5].

High gain power converters are important components in photovoltaic systems due to the following reasons:

1. They boost low PV voltages to higher levels.
2. They make voltage conversion more efficient.
3. The help reduce switching losses and stress on the voltage.
4. They facilitate effective MPPT control.

1.2 Literature Survey

Due to an increase in the popularity of renewable energy systems, a lot of attention is being paid towards high gain DC-DC converters and MPPT methods used with photovoltaic (PV) systems. Research has been conducted in terms of voltage conversion, power harvesting efficiency, response time, and reliability under different environmental conditions.

In Bose [4], a survey was conducted on the history of power semiconductor devices and its effect on converter development. The paper focused on the significance of advanced semiconductor devices in switching operation of converters to enhance power losses as well as converter efficiency. It also pointed out future advancements in the area of converters design, focusing on miniaturization.

The paper Imbertson and Mohan [6] provided a technique of calculating physical dimensioning of switch-mode power supplies. According to the results, the converter topology, operating frequency, and the magnetic part have a significant effect on the size of converters.

The inadequacies of traditional boost converters have led to the emergence of high gain converter topologies. In his study, Bose [7] addressed the influence of semiconductor devices' properties on the performance of converters and identified trends in power conversion technology for the future. With an increasing demand for converters with significant voltage gain in renewable energy applications, attention has been drawn towards designing converters capable of providing a high voltage gain at low duty cycles.

The following are some of the notable contributions that have recently been made regarding high gain converters designed for renewable energy applications. In their research work, Gopinathan et al. [8] proposed a novel class of non-isolated quadratic converters with high gain that incorporates extended capacitor diode circuits. These topologies enable voltage gain while keeping semiconductor device voltages low enough. Moreover, the suggested topologies exhibit high efficiency and better power processing abilities than traditional boost converters.

Still, the size of a converter as well as the power density is crucial for energy systems with renewables. Imbertson and Mohan [9] researched the way of estimating the physical size of a switch mode power supply, paying attention to the interplay between converter topology and switching frequency in relation to power component sizing. The results achieved contributed significantly to developing a compact and high-performance design of the converters used in modern energy systems.

In the context of the growing transition from fuel-fired generation to renewable energy sources, there arises the need for efficient PV power conversion systems. According to Mutezo and Mulopo [10], who studied the use of renewable energy in terms of circular economy concepts, improvements in energy conversion are needed to ensure sustainable development. Photovoltaic systems were found to be among the driving forces behind the global energy transition.

MPPT technique is an essential element of photovoltaic energy system due to the variability of PV modules' operation depending on solar irradiance and temperature. As for conventional MPPT algorithms such as P&O and Increamental conductance, they became popular due to their simplicity and straightforwardness of implementation.

From the above literature review, one can clearly observe the advancement that has been achieved in terms of designing high gain dc-dc converters as well as the MPPT methods used in photovoltaics. Even though the standard boost converter topology is still widely preferred due to its simplicity, its limitations have promoted the emergence of high gain converters like quadratic converters and many others. At the same time, there is continued development of MPPT schemes to guarantee maximum power output under different environmental conditions.

1.3 Research Gaps

It is evident from the reviewed literature that traditional boost converters cannot provide adequate performance in applications that need high voltage gain due to the dependency of the former on high duty cycles, which in turn results in efficiency loss. While several converters that yield high voltage gain have been introduced, most of them employ a large number of components, thereby resulting in complex systems. Moreover, the integration of high-gain converters with efficient MPPT control strategies is still a topic of current research interest. As can be observed from the literature review, many scholars concentrated their efforts on achieving increased voltage gain, reduction in switching stress, and high efficiencies in converters. While several quadratic boost converter configurations exist, more research is needed in order to improve the performance of the converter in different levels of irradiation for photovoltaic systems. For these reasons, the purpose of this dissertation is to design and simulate the operation of a quadratic boost converter coupled with MPPT controller that will offer a high voltage gain from photovoltaic solar cells.

Consequently, this paper aims at designing and implementing a quadratic boost converter in conjunction with the Perturb and Observe MPPT control scheme for PV systems. Thus, the current study is concerned with the development of a quadratic boost converter along with the Perturb and Observe MPPT control strategy. The objective of the developed system is to obtain high voltage gain, efficiency, and maximum power extraction capability under different solar insolation conditions.

1.4 Thesis Objectives

The main aim of this research work is to study the use of quadratic boost converters for the photovoltaic power generation systems and to examine their effectiveness in giving high-voltage conversion ratios without losing power transfer efficiency.

The objectives of this study include the following:

1. To design a quadratic boost converter for photovoltaic applications with high voltage conversion ratios.
2. To investigate the performance of the suggested converter in improving output voltage and maximizing energy consumption from the solar cell.

3. In order to investigate the comparative performances of quadratic boost converters and ordinary boost converters and analyze the merits of the suggested topology.

4. In order to establish the suitability of quadratic boost converters in renewable energy applications where high voltage gain is essential.

CHAPTER 2

Quadratic Boost DC-DC Converter

The reviewed literature indicates that quadratic boost converters provide significantly higher voltage gain than conventional boost converters while maintaining lower switch stress and improved efficiency. Various researchers have proposed modified topologies such as double-inductor structures, voltage multiplier cells, and single-switch configurations to further improve converter performance. Additionally, integrating MPPT techniques with quadratic boost converters enhances power extraction from photovoltaic systems under varying irradiance conditions. Therefore, the quadratic boost converter is considered an effective solution for renewable energy applications requiring high-gain DC–DC power conversion.

In his paper, M. Veerachary introduced a novel design of a quadratic boost converter for high step-up DC–DC converters. The converter aimed to have a greater voltage ratio than the traditional boost converter while maintaining low values of duty ratio. The research included analysis of the circuit, derivation of the transfer function, and formulation of a state space model of the converter. From the study, it is evident that the novel circuit had better voltage boosting ability coupled with lower voltage stress on the switch [7].

Balal and F. Shahabi proposed a double-inductor quadratic boost converter and analyzed its performance using LTspice simulation software. The converter was compared with conventional quadratic boost and double cascaded boost converter topologies. The results demonstrated that the double-inductor structure improved voltage gain and efficiency while reducing switching losses. The study also showed better current handling capability and enhanced converter performance under high-voltage operating conditions. The proposed topology achieved improved output characteristics and stable operation in both transient and steady-state conditions [8].

A photovoltaic energy conversion system using a quadratic boost converter in combination with an MPPT controller has been designed by N. Altin and E. Ozturk. The INC technique was used for the tracking of maximum power point in a situation where solar irradiation varies. The suggested converter not only succeeded in stepping up the low voltage output from the PV module but also extracted maximum possible power. The simulation and experimental results clearly indicated that the system worked efficiently and successfully tracked the maximum power point despite changing environmental conditions [9].

D. Anusha, S. Youvaraj, G. Youvaraj, H. Bhanarkar, B. Marupatla, and S. Pradabane designed a modified single switch quadratic boost converter for renewable energy applications. The circuit was intended to provide high voltage gain with lower duty cycles while minimizing stresses on components and switching losses. Simulation results using MATLAB showed that there was an improvement in output voltage performance, efficiency, and stability of the converter. The simplicity introduced by the design, especially the use of a single switch, made the circuit easy to implement [10].

2.1 Introduction

When you are modelling a quadratic boost converter that is working in conduction mode you need to include the losses and component imperfections in the duty cycle and voltage gain equations. This helps you get accurate design results. Considering these -ideal effects helps improve the reliability, efficiency and practical implementation of DC-DC converters, in real-world power electronic applications.

$$\frac{Vo}{Vs} = \frac{1}{(1-D)^2} \qquad 2.1$$

The Quadratic Boost converter has an output voltage, which we call Vo and an input voltage, which we call Vs for the Quadratic Boost converter.

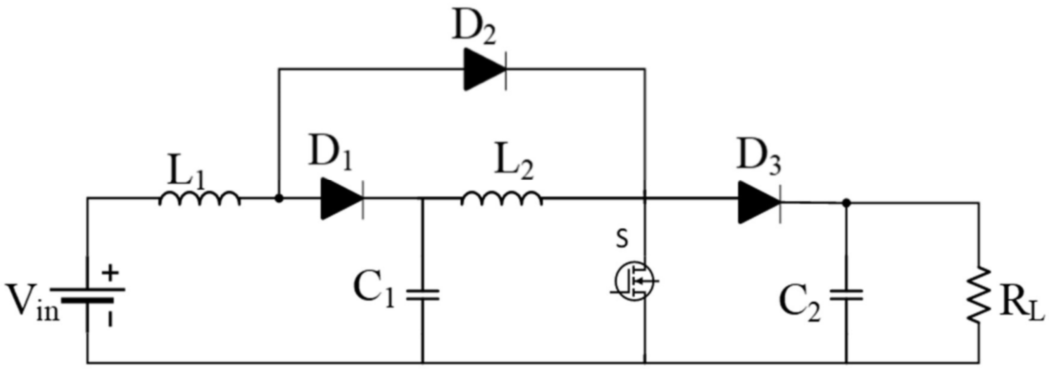

Fig 2.1: Schematic Diagram of Quadratic Boost Converter.

2.2 Analysis of Quadratic Boost DC-DC Converter

The picture of a quadratic boost DC-DC converter in Figure 2.1 shows a setup. This setup is used to control voltage levels. The quadratic boost DC-DC converter has two inductors, two capacitors, three diodes and a switch. The switch is usually a transistor. The quadratic boost DC-DC converter uses these parts to move energy from the input side to the output side. The inductors and capacitors in the boost DC-DC converter are important because they store energy. They help make sure the voltage and current stay steady. This is necessary for the quadratic boost DC-DC converter to have an output. The quadratic boost DC-DC converter is special because it can adapt to situations. This is what makes the boost DC-DC converter different, from other converters. This versatility is evidenced by the fact that it can operate in two modes: Continuous Conduction Mode (CCM) and Discontinuous Conduction Mode (DCM). For the purposes of this investigation, the operations of the CCM are the primary focus of attention. When it comes to understanding how the converter operates under steady conditions, this mode is necessary, with a particular emphasis placed on the duty cycle (D) and the switching frequency (fs). Due to the fact that the duty cycle, which is defined as the ratio of the active time of the switch to the entire cycle time, is an essential component in the process of controlling the output of the converter, we have incorporated it into our analysis. Mathematically,

$$D = \frac{Ton}{Ton+Toff} = \frac{Ton}{Ts} = \text{Ton.fs} \qquad 2.2$$

Where, Ton = time of interval when the MOSFET = ON and Toff =time interval when MOSFET (s) = OFF.

From Eqn. (2.2), We get,

$$\text{Ton} = \text{DTs (When MOSFET = ON)} \qquad 2.3$$

$$\text{Toff} = (1 - \text{D})\text{Ts (When MOSFET = OFF)} \qquad 2.4$$

Quadratic Boost converter is controlled by MOSFET switching mechanisms. In CCM mode it has two switching mode (a) When the MOSFET is ON and the Diode is turned OFF, or (b) When the MOSFET is turned OFF and the Diode Conducts.

2.3 Mode I Operation (0 < t < DTs)

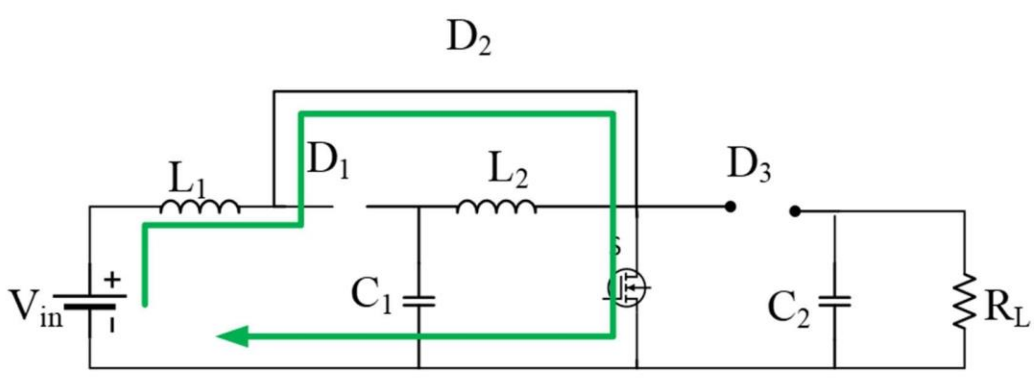

Fig 2.2: Schematic Diagram of Quadratic Boost during MODE I Operation.

When referring to a Quadratic Boost DC-DC converter, the phase known as Mode 1 is the phase in which the MOSFET is activated and the diodes D1 and D3 are non-conducting, while the diode D2 is conducting. During the process of turning on the MOSFET in Mode 1, the current travels through an inductor, L1, the MOSFET, and finally to the ground. The voltage that is placed across inductor L1 causes the current that flows through it to grow in a linear fashion with the passage of time. More energy is stored in inductor L1 as a result of the energy it receives from the input voltage source. Due to the fact that it is storing energy from the previous cycle, the capacitor C2 begins to discharge through the closed MOSFET at this point in time. As a result, the voltage across C2 gets lower.

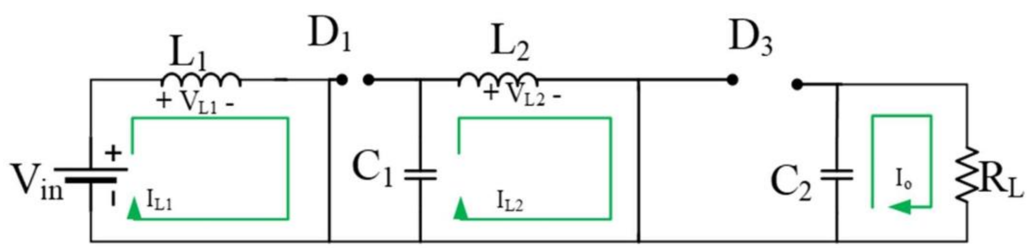

Fig 2.3: Equivalent Circuit Diagram for MODE I Operation.

Using Kirchoff's law of voltage and current, the voltage across the inductor L1 and L2, the current across the capacitor C1 and C2, and the output voltage may be calculated as follows:

$$V_{L_1,on} = L_1 \frac{di_{L_1}}{dt} = V_s \qquad 2.5$$

$$V_{L_2,on} = L_2 \frac{di_{L_2}}{dt} = V_c \qquad 2.6$$

$$i_{C_1,on} = C_1 \frac{dV_{C_1}}{dt} = i_{L_2} \qquad 2.7$$

$$i_{C_2,on} = C_2 \frac{dV_{C_2}}{dt} = -\frac{V_o}{R_o} \qquad 2.8$$

$$V_o = V_{C_2} \qquad 2.9$$

2.4 Mode II Operation (DTs < t < (1 − D)Ts)

Changes occur in the dynamics of the system during the second stage of the Quadratic Boost converter, which occurs when the MOSFET is turned off. It is observed that the diodes D1 and D3 begin to conduct, however the diode D2 fails

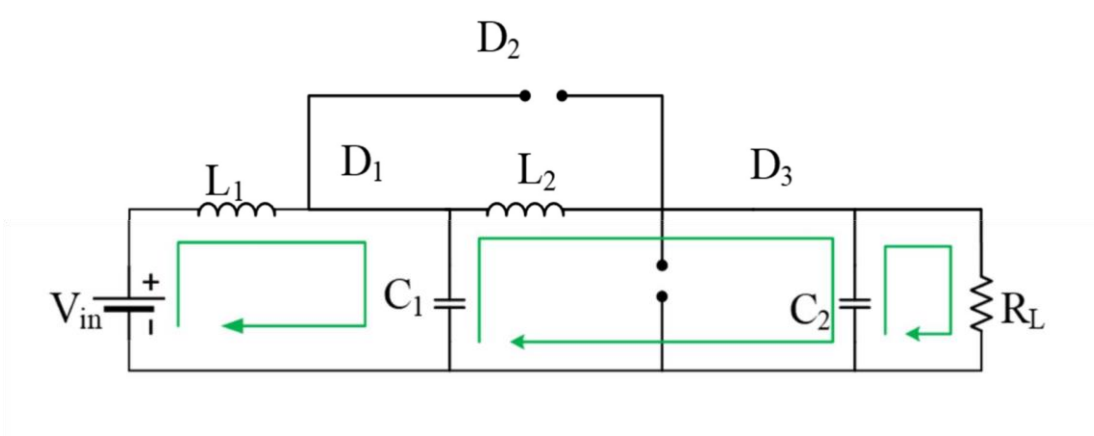

Fig 2.4: Schematic Diagram of Quadratic Boost during MODE II Operation.

to conduct. Currently, the inductor L1, which had been accumulating current, is now forcing that current through diodes, which begin to conduct as a result of the MOSFET's lack of activity. This current then continues on to charge capacitor C1, and the energy that was stored in L2 is transmitted to the output capacitor C2 as well as the load. The two different modes of functioning are depicted in Figure 2.4.

Using Kirchoff's law of voltage and current, the voltage across the inductor L1 and L2, the current across the capacitor C1 and C2, and the output voltage may be calculated as follows:

$$V_{L_2,off} = L_2 \frac{di_{L_2}}{dt} = V_{C_1} - V_{C_2} \quad 2.11$$

$$i_{C_1,off} = C_1 \frac{dV_{C_1}}{dt} = i_{L_1} - i_{L_2} \quad 2.12$$

$$i_{C_2,off} = C_2 \frac{dV_{C_2}}{dt} = i_{L_2} - \frac{V_{C_2}}{R_o} \quad 2.13$$

$$V_O = V_{C_2} \quad 2.14$$

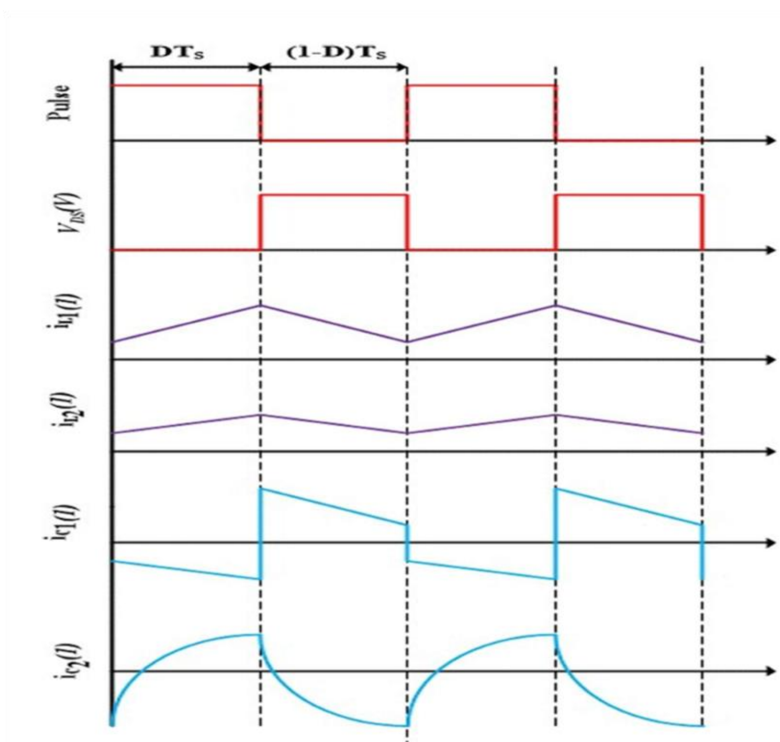

Fig 2.5: Switching waveform for Quadratic Boost converter.

2.5 Steady State Analysis.

In the context of steady-state analysis, the mean value of a current and voltage variable, denoted as x can be described as follows:

$$X = \frac{1}{T}\int_0^T x(t)dt = \frac{1}{T}\int_0^{DT} xon(t)dt + \frac{1}{T}\int_{DT}^T xoff(t)dt \qquad 2.15$$

Where xon and xoff denotes the variable x(t) when switch is on and off respectively.

According to the principle of volt-second balance for an inductor, over a full cycle of a switched-mode power supply, the cumulative voltage applied to an inductor equals zero i.e,

$$V_L = \frac{1}{T}\int_0^T vL(t)dt = \frac{1}{T}\int_0^{DT} vLon(t)dt + \frac{1}{T}\int_{DT}^T vLoff(t)dt = 0 \qquad 2.16$$

Similarly, as per the Ampere-Second balance for a capacitor, over a complete switching cycle, the net charge transferred to and from a capacitor equals zero, signifying a state of dynamic equilibrium. This is given by:

$$Ic = \frac{1}{T}\int_0^T ic(t)dt = \frac{1}{T}\int_0^{DT} ic,on(t)dt + \frac{1}{T}\int_{DT}^T ic,off(t)dt \qquad 2.17$$

Also, the average output voltage of the Quadratic Boost converter is given by:

$$V_0 = \frac{1}{T}\int_0^T v0(t)dt = \frac{1}{T}\int_0^{DT} v0,on(t)dt + \frac{1}{T}\int_{DT}^T v0,off(t)dt \qquad 2.18$$

2.6 Expression for output Voltage

The output voltage of Quadratic Boost Converter can be determined by applying volt-second balance to the inductor L1. By substituting equation 2.5 and equation 2.10 into equation 2.16, we obtain:

$$\frac{1}{T}\int_0^{DT} vs(t)dt + \frac{1}{T}\int_{DT}^{T}(Vs - Vc1)dt \ = 0 \qquad 2.19$$

On simplifying the eq.2.19 we get,

$$VsD + (1\text{-}D)(Vs\text{-}Vc1) = 0 \qquad 2.20$$

$$Vs - (1 - D)Vc1 = 0 \qquad 2.21$$

Similarly, the average Voltage of capacitor C1 can be calculated by applying KVL from voltage source to the output voltage,

$$Vc1 = Vc2 - DVc2 \qquad 2.22$$

Substituting the value from eq.(2.21) to eq.(2.22), we get

$$\frac{Vo}{Vs} = \frac{1}{(1-D)^2} \qquad 2.23$$

Table 1.1: Specification of Quadratic Boost converter.

Parameters	Values
I/P Voltage Vs	12V
O/P Voltage Vo	48V
Load Resistance Ro	23.04Ω
Inductance L1	145μH
Inductance L2	576 μH
Capacitor C1	200 μF
Filter Capacitor C2	470 μF
Switching Frequency fs	50KHz
Desired Inductor Current RippleΔiL1/Δ iL2	10%IL1/10%IL2
Desired Output Voltage Ripple Current Ripple ΔVc1/ΔVc2	1%Vc1/1%Vc2

2.7 Inductor Current Ripple and Inductor Design.

The design of inductors is crucial to the efficiency of DC-DC converters. It affects their efficiency, dimensions, and regulation of voltage variations. Inductors are pivotal in the storage and transfer of energy, influencing the overall performance of the converter. Consequently, prioritizing innovation in inductor design is crucial for attaining more efficient, compact, and resilient DC-DC converters.

Let ΔiL1 and ΔiL2 be the desired ripple in inductor current (ICR) and xL1 and xL2 be the desired inductor current ripple factor (ICRF) for both the inductors. The relationship between the ICR and ICRF is given by:

$$xL1 = \frac{\Delta iL1}{iL1} \quad 2.24$$

Similarly,

$$xL2 = \frac{\Delta iL2}{iL2}$$

Where, IL1 and IL2 are the average currents flowing through inductor L1 and L2.

Now, under steady state, using eq. (2.5), it can be written as,

$$L1\frac{diL1}{dt} = Vs \quad 2.25$$

By substituting the switch on duration, dt = DTs, we get,

$$L1 = \frac{Vs+DTs}{\Delta iL1} \quad 2.26$$

Since Ts = 1/fs, therefore eq.2.27 can be rewritten as,

$$L1 = \frac{Vs*D}{\Delta iL1*fs} \quad 2.27$$

Similarly for Inductor

$$L2 = \frac{Vs*D}{(1-D)\Delta iL2*fs} \qquad 2.28$$

2.8 Output Voltage Ripple and Capacitor Design.

The capacitor is an important part of a DC-DC converter system. It really helps to make the voltage more stable and reduces the noise in the system. The capacitor stores. Then releases it, which helps to keep the voltage steady and reduces interference from other parts of the circuit.

The capacitor you choose is very important for the converter to work well. You need to pick a capacitor with the capacitance value, voltage rating and size for your converter. If you choose the capacitor it will help to keep the voltage steady make the converter more reliable and make the whole system work more efficiently. So choosing the capacitor is crucial for a quadratic boost DC-DC converter to work properly.

When the system is working steadily let us say we want the voltage to ripple by an amount, across the capacitors C1 and C2.

We can use equation 2.7 to figure this out. We need to consider the average current flowing through the inductor current iL2, we get

$$Qc1 = C1\Delta Vc1 \qquad 2.29$$

$$C1 = \frac{I0.D.Ts}{(1-D).\Delta Vc1} \qquad 2.30$$

$$C1 = \frac{V0.D}{(1-D).\Delta Vc1.fs.R0} \qquad 2.31$$

Similarly for Inductor C2,

$$C2 = \frac{V0.D}{.\Delta Vc2.fs.R0} \qquad 2.32$$

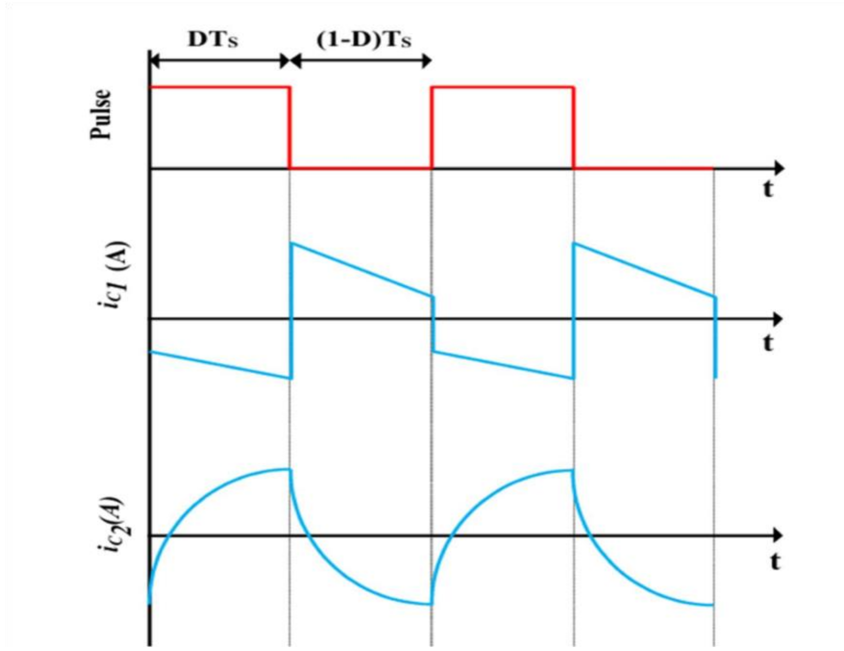

Fig 2.6: Charging and Discharging Behaviour of Capacitor C1 and C2.

2.9 Result and Discussion.

The effective design of a Quadratic Boost converter was theoretically developed and simulated in MATLAB Simulink. To this end, all simulation parameters were taken. In the course of the simulation, various output voltage response scenarios were modelled in order to assess the theoretical performance of the Quadratic Boost converter by way of results that could be compared and contrasted with the predicted output responses. The results of the simulated performance were consistent with the output prediction methods used in the theoretical design of the Quadratic Boost converter, providing a linear relationship between duty cycle increase and output voltage increase, and vice versa when duty cycle is decreased.

The Quadratic Boost converter's output voltage was maintained at 48 volts when operated under no load, as specified by equation 2.2, with a calculated duty cycle of 0.5 based on relationship between input and output voltages defined in equation 2.1 and with each of the two inductances (L1 and L2) having been specifically designed to have values of 0.145mH and 0.576mH respectively.

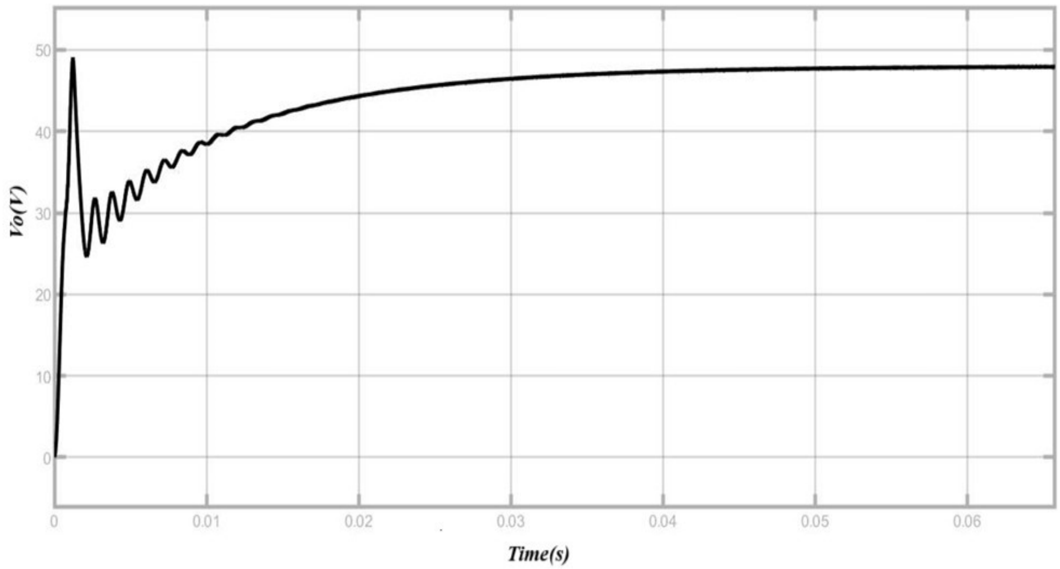

Fig 2.7: Output Voltage response at rated condition.

The Quadratic Boost converter has been aged sufficiently to allow an accurate representation of its actual performance characteristics, producing an efficient and stable output voltage of 48 volts in an open loop operating mode.

This capability to regulate an output voltage accurately (in an open-loop system) demonstrates how well the converter is designed and built. An interesting relationship exists between Output Voltage and Switching Frequency as illustrated in Figure 2.9. As Switching Frequency increases, a corresponding decrease in Output Voltage Ripple can also be seen. Since the trend clearly shows that by increasing Switching Frequency, Output Quality can be improved, this is a very important inverse relationship for applications requiring a smooth DC Output.

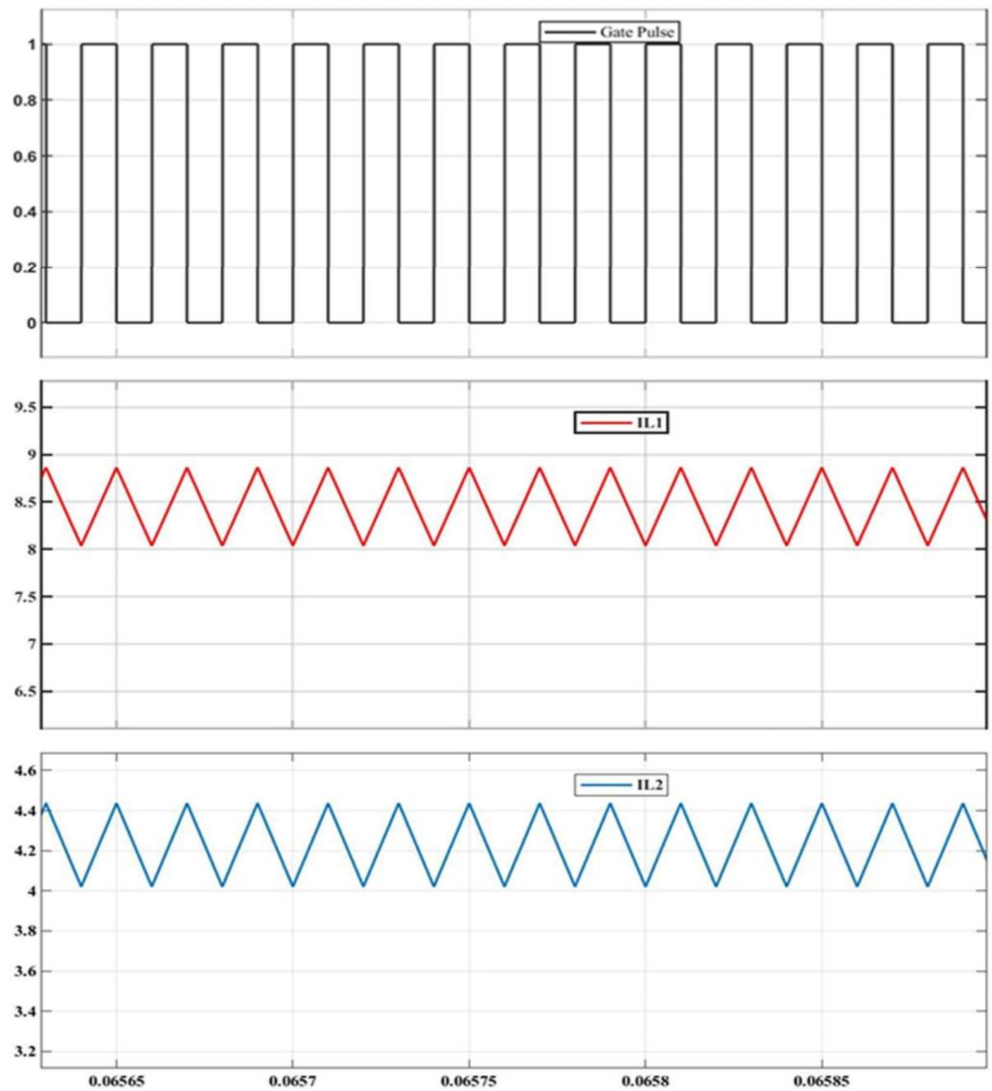

Fig 2.8: Current Profile of Inductor L1 and L2.

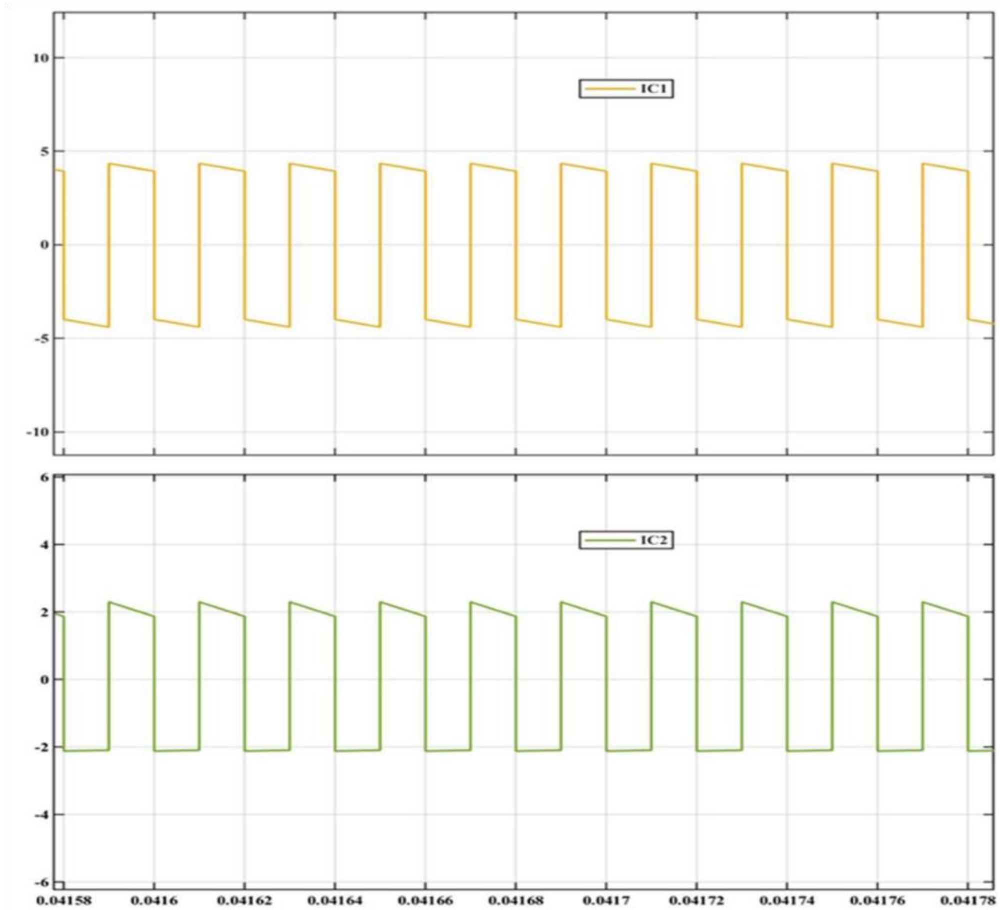

Fig 2.9: Current Profile of Capacitor C1 and C1.

Another fascinating relationship between the value of inductance and the frequency of switching is illustrated in Figure 2.11. Data shows that as you increase the number of times that you switch, you will find that you have less inductance than if you had no switching. The current data collected through this study has an impact on the physical design of Compact Quadratic Boost converters. The higher your frequency of switching the smaller the inductor you will use, therefore; you should be able to decrease both the cost and size of your inductor without having any negative impact on performance measures.

CHAPTER 3

MODELLING OF DC-DC CONVERTERS

3.1 Introduction

The modelling of DC to DC or direct current to direct current converters, is arguably the first step to designing high efficiency power conversion systems. There is great value in modelling since it provides engineers and designers insight into how the converters are likely to perform under various conditions. Engineers and designers can optimise converter performance and increase efficiency, as well as provide reliable product performance in real-world conditions, when they have a solid understanding of how converters react to various load levels, input voltages, and environmental conditions, as well as developing a controller that can accurately regulate the output voltage or output current, keep the output stable in dynamic conditions, and appropriately respond to disturbances in output voltage/current.

Of particular significance are applications that require high efficiency power conversion and high-speed responsiveness, including automotive, portable electronics, and renewable energy systems. The use of state-space averaging techniques, as discussed throughout this thesis, is used to model converters because it provides a straightforward method for explaining the system's dynamics, while at the same time providing a reasonably accurate representation of the system's performance characteristics. State-space averaging techniques provide a means of simplifying the complex behaviour of electrical systems into a form that is easier to work with and evaluate for controller design.

3.2 State Space averaging Modelling Technique

The state-space averaging technique models and analyzes the dynamic behaviour of power converters. This method transforms the nonlinear, switching nature of DCDC converters into linear time-invariant (LTI) systems throughout a transitioning time. This allows for the use of linear control theory to develop and analyze converter controllers, making it easier and faster than dealing with nonlinear systems.

The method is made up of many steps. The first thing it does is figure out the converter's states (like "on" and "off") and model their circuit equations in state-space form. The duty cycle of the converter is used to average the state-space equations for one switching time. This makes a set of average state-space equations that describe how the translator behaves over time. State-Space Averaging permits a comprehensive and holistic view of DC-DC converter performance/connection between an electrical and control system. The complete picture enables the design/engineering functions of a converter to improve overall reliability through the integrated combination of the electrical component with the control system component.

Using state-space averaging, engineers can develop models that depict both ideal and non-ideal DC-DC converters' real-world performance. As a result, efficient and robust power conversion systems/controllers can be engineered/constructed. The state-space averaging technique simplifies the analysis and design of power electronic converters by reducing their nonlinear behaviour to linear time-invariant (LTI) models. The steps below demonstrate the generalized state space averaging modelling technique.

Step 1: Identify System States

The initial stage is to determine the several operational states of the converter. For a conventional switched-mode power supply, these states relate to the switching components (such as MOSFETs or diodes) being in either an 'on' or 'off' condition. Every operating condition of the DC-DC converter is characterized by its own set of system equations. Usually, the state variables chosen for modelling are the currents running through inductors and the voltages across capacitors. The total number of state variables therefore directly depends on the quantity of inductors and capacitors in the circuit. A state variable vector, represented as x(t), encapsulates these state variables.

The state equations for the two operational circuit states under Continuous Conduction Mode (CCM) can be stated as follows:

I. When the MOSFET is on during the switching interval 0 < t < DT, the state equation is given as:

$$\frac{dx(t)}{dt} = A1x(t) + B1u(t) \qquad 3.1$$

$$y(t) = E1x(t) + F1u(t) \qquad 3.2$$

II. When the MOSFET is off during the switching interval DT < t < T, the state equation is given as:

$$\frac{dx(t)}{dt} = A2x(t) + B2u(t) \qquad 3.3$$

$$y(t) = E2x(t) + F2u(t) \qquad 3.4$$

x(t) represents the state variable vector, encompassing inductor currents and capacitor voltages, with the controllable input indicated as u(t) and the output vector as y(t). The state matrix is represented as A, the input matrix as B, the output matrix as E, and the output coupling matrix as F.

Step 2: State Space Averaging equation:

Averaging the state equations across one switching period for every state variable, considering the duty cycle. Averaging over one switching interval removes the switching ripple component from the circuit equations. To analyse and design by means of linear control theory, you can multiply the equations of state in the 'on' state by D and then multiply the 'off' equations by 1 - D and then sum them. This way of linearising the model allows for analysis and design using linear control theory.

$$\frac{d\bar{x}(t)}{dt} = A\bar{x}(t) + B\bar{u}(t) \qquad 3.5$$

$$\bar{y}(t) = C\bar{x}(t) + D\bar{u}(t) \qquad 3.6$$

Where,

$$A = A_1 * d(t) + A_2 * \left(1 - d(t)\right) \qquad 3.7$$

$$B = B_1 * d(t) + B_2 * (1 - d(t)) \tag{3.8}$$

$$E = E_1 * d(t) + E_2(1 - d(t)) \tag{3.9}$$

$$F = F_1 * d(t) + F_2(1 - d(t)) \tag{3.10}$$

The overline (-) shows that a variable's average value has been measured from a continuous transition across the course of an entire switching cycle in relation to the state space (averaged) model structure. The equations (3.5) and (3.6) exhibit non-linear characteristics caused by the multiplication of time varying variables within these same two equations.

Step 3: Average State Space Model Perturbation and Linearization

The use of perturbation/linearization techniques is common when analyzing and controlling dynamic systems that exhibit non-linear properties, as found in the averaged state-space models. Perturbations are created by applying small deviations from a steady state operating point, which helps to provide an approximate representation of the dynamic characteristics of the system. This technique provides a means of identifying control strategies and performing analysis on dynamic systems, particularly for the power electronics community.

The small ac perturbation introduced around steady state values are as follows:

$$\bar{x}(t) = X + \hat{x}(t)\ , \bar{y}(t) = Y + \hat{y}(t)$$
$$d(t) = D + \hat{d}(t), \quad d'(t) = 1 - d(t) = 1 - D - \hat{d}(t) = D' - \hat{d}(t) \tag{3.11}$$

It is to note that $X \gg \hat{x}(t), Y \gg \hat{y}(t), U \gg \hat{u}(t) and\ D \gg \hat{d}(t)$.

By substituting the eq. (3.11) into eq. (3.5) -(3.6) we get,

$$\dot{X} + \dot{\hat{x}}(t) = \left[A_1\left(D + \hat{d}(t)\right) + A_2\left(1 - D - \hat{d}(t)\right)\right](X + \hat{x}(t)) + \left[B_1\left(D + \hat{d}(t)\right) + B_2\left(1 - D - \hat{d}(t)\right)\right](U + \hat{u}(t)) \tag{3.12}$$

On simplifying, we get

$$\dot{X} + \dot{\hat{x}}(t) = [A_1 D + A_2(1 - D) + (A_1 - A_2)\hat{d}(t)](X + \hat{x}(t)) + [B_1 D + B_2(1 - D) + (B_1 - B_2)\hat{d}](U + \hat{u}(t)) \tag{3.13}$$

Similarly

$$Y + \hat{y}(t) = \left[E_1\left(D + \hat{d}(t)\right) + E_2\left(1 - D - \hat{d}(t)\right)\right](X + \hat{x}(t)) + \left[F_1\left(D + \hat{d}(t)\right) + F_2\left(1 - D - \hat{d}(t)\right)\right](U + \hat{u}(t)) \quad 3.14$$

Simplifying the above equation yield

$$Y + \hat{y}(t) = [E_1 D + E_2(1 - D) + (E_1 - E_2)\hat{d}(t)](X + \hat{x}(t)) + [F_1 D + F_2(1 - D) + (F_1 - F_2)\hat{d}](U + \hat{u}(t)) \quad 3.15$$

To formulate the linear model, we exclude the second-order nonlinear factors that result from the multiplication of two minor AC perturbed signals, as indicated in equations (3.13) to (3.15). Consequently, we derive:

$$\dot{X} + \hat{\dot{x}}(t) = (A_1 D + A_2(1 - D))X + (A_1 D + A_2(1 - D))\hat{x}(t) + (A_1 - A_2)X\hat{d}(t) + (B_1 D + B_2(1 - D))U + (B_1 D + B_2(1 - D))\hat{u}(t) + (B_1 - B_2)U\hat{d}(t) \quad 3.16$$

$$Y + \hat{y}(t) = (E_1 D + E_2(1 - D))X + (E_1 D + E_2(1 - D))\hat{x}(t) + (E_1 - E_2)X\hat{d}(t) + (F_1 D + F_2(1 - D))U + (F_1 D + F_2(1 - D))\hat{u}(t) + (F_1 - F_2)U\hat{d}(t) \quad 3.17$$

Now the above equations can be written as:

$$\dot{X} + \hat{\dot{x}}(t) = AX + BU + A\hat{x}(t) + B\hat{u}(t) + [(A_1 - A_2)X + (B_1 - B_2)U]\hat{d}(t) \quad 3.18$$

$$Y + \hat{y}(t) = EX + FU + E\hat{x}(t) + F\hat{u}(t) + [(E_1 - E_2)X + (F_1 - F_2)U]\hat{d}(t) \quad 3.19$$

$$Where\ , A = A_1 D + A_2(1 - D), B = B_1 D + B_2(1 - D), E = E_1 D + E_2(1 - D), F = F_1 D + F_2(1 - D) \quad 3.20$$

3.3 Small Signal AC Model

Separating out the small signal ac terms from eq. (3.18) -(3.19), we get

$$\hat{\dot{x}} = A\hat{x}(t) + B\hat{u}(t) + [(A_1 - A_2)X + (B_1 - B_2)U]\hat{d}(t) \quad 3.21$$

$$\hat{y}(t) = E\hat{x}(t) + F\hat{u}(t) + [(E_1 - E_2)X + (F_1 - F_2)U]\hat{d}(t) \quad 3.22$$

To ascertain the various transfer functions, we employ the Laplace transform on the previously given state-space model, resulting in the following expression:

$$s\hat{x}(s) = A\hat{x}(s) + B\hat{u}(s) + [(A_1 - A_2)X(s) + (B_1 - B_2)U(s)]\hat{d}(s) \qquad 3.23$$

$$\hat{y}(s) = E\hat{x}(s) + F\hat{u}(s) + [(E_1 - E_2)X(s) + (F_1 - F_2)U(s)]\hat{d}(s) \qquad 3.24$$

Equations (3.23) and (3.24) provide the foundation for deriving various transfer functions pertinent to DC-DC converters. In the context of a DC-DC converter, the variable (x) pertains to the oscillations in inductor current and capacitor voltage, whereas (u) relates to changes in input voltage and load current. The symbol (d) denotes variations in the duty cycle, while (y) represents modifications in the output voltage. Through the analysis of these equations, we may get the transfer functions that delineate the link between these perturbations as specified in Equations (3.25) - (3.26).

The transfer functions relating the duty cycle (d) and the input variables (u) to the state variables (x) have been defined as follows:

$$\frac{\hat{x}(s)}{\hat{d}(s)} = (sI - A)^{-1}[(A_1 - A_2)X(s) + (B_1 - B_2)U(s)] \qquad 3.25$$

$$\frac{\hat{x}(s)}{\hat{u}(s)} = (sI - A)^{-1}B \qquad 3.26$$

The relationships between the duty cycle (d) and the input parameters (u) to the output response (y) are represented by a series of transfer functions.

$$\frac{\hat{y}(s)}{\hat{d}(s)} = E(sI - A)^{-1}[(A_1 - A_2)X(s) + (B_1 - B_2)U(s)] + [(E_1 - E_2)X + (F_1 - F_2)U] \qquad 3.27$$

$$\frac{\hat{y}(s)}{\hat{u}(s)} = E(sI - A)^{-1}B + F \qquad 3.28$$

The transfer functions for Quadratic Boost Converter will be derived in the sections below.

3.4 Modelling of Quadratic Boost Converter

To model a Quadratic Boost Converter, an understanding of the underlying basic circuit design is beneficial, which relates to the discussion in the previous chapter. The circuit has time-variant electrical characteristics and exhibits AC-like transient relationships of current and voltage. Significantly, an additional current source, called z(t), has been incorporated into the output stage of the converter, and it provides for the evaluation of the effects of changing load currents on output voltage response.

This document focuses on modelling a DC to DC Quadratic Boost Converter. It is assumed that the converter will be functioning within CCM. A DC to DC Quadratic Boost Converter will switch between two different modes of operation CCM: (a) the MOSFET switch is in an 'on' state (conducting) and the diode is in an 'off' state (not conducting), and (b) the MOSFET switch will have transitioned from an 'on' state (conducting) to an 'off' state (not conducting), and has now transitioned to an 'off' state (not conducting) and the diode is now conducting (on). The state-space equations for two operations of the converter will be derived in order to gain further insight into the performance of the converter.

Step 1: Identifying System States and obtain the state space equations.

I. Switch ON duration (0 < t < DT)

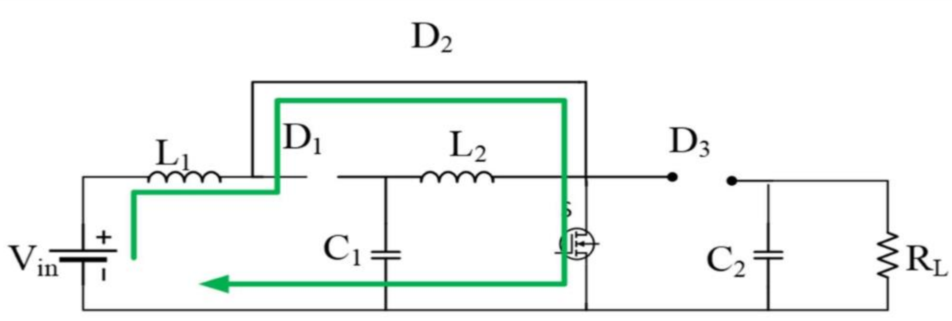

Fig 3.1: Circuit Diagram when Switch ON (MODE I).

The starting condition entails the switch, often a MOSFET, being in a closed position. This action facilitates energy transfer from the input source, through the inductors, and into the capacitors. According to Kirchhoff's voltage and current laws, the equations for inductor voltage, capacitor current, and output voltage are expressed as follows:

$$V_{L_1}(t) = L_1 \frac{di_{L_1}(t)}{dt} = V_s(t) \qquad 3.29$$

$$V_{L_2}(t) = L_2 \frac{di_{L_2}(t)}{dt} = V_{C1}(t) \qquad 3.30$$

$$i_{C_1}(t) = C_1 \frac{dV_{C_1}(t)}{dt} = i_{L_2}(t) \qquad 3.31$$

$$i_{C_2}(t) = C_2 \frac{dV_{C_2}(t)}{dt} = -\frac{V_{C2}(t)}{R_o} \qquad 3.32$$

$$V_o = V_{C_2}(t) \qquad 3.33$$

Equations eq.(3.29)-eq.(3.33) can be written in state-space representation as:

$$\begin{bmatrix} \frac{di_{L_1}}{dt} \\ \frac{di_{L_2}}{dt} \\ \frac{dV_{C_1}}{dt} \\ \frac{dV_{C_2}}{dt} \end{bmatrix} = A_1 \begin{bmatrix} i_{L_1} \\ i_{L_2} \\ V_{C_1} \\ V_{C_2} \end{bmatrix} + B_1[V_s] \qquad 3.24$$

$$[V_o] = E_1 \begin{bmatrix} i_{L_1} \\ i_{L_2} \\ V_{C_1} \\ V_{C_2} \end{bmatrix} + F_1[V_s] \qquad 3.35$$

Where,

$$A_1 = \begin{bmatrix} 0 & 0 & 0 & 0 \\ 0 & 0 & 1 & -\frac{1}{L_2} \\ 0 & -\frac{1}{C_1} & 0 & 0 \\ 0 & 1 & 0 & \frac{-1}{R_o C_2} \end{bmatrix}, B_1 = \begin{bmatrix} \frac{1}{L_1} \\ 0 \\ 0 \\ 0 \end{bmatrix} \quad 3.36$$

$$E_1 = [0 \quad 0 \quad 0 \quad 1]\,, F_1 = [0]$$

ii. Switch OFF duration (DT< t < T)

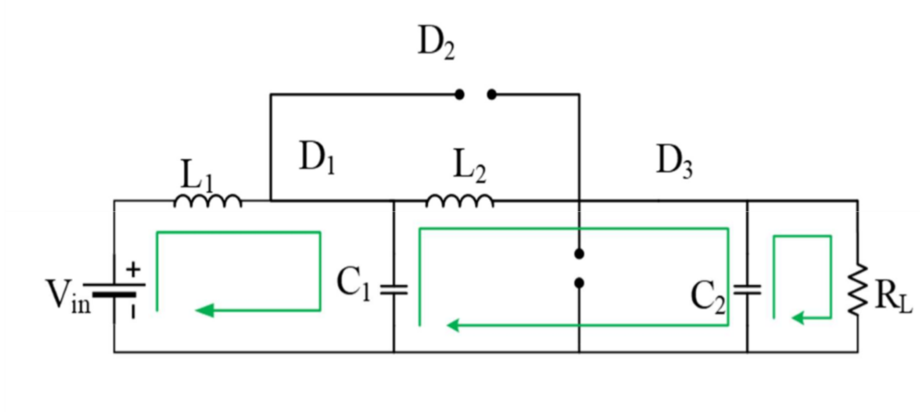

Fig 3.2: Circuit Diagram when Switch OFF (MODE II).

The diode conducts in the following state when the MOSFET switch is opened. A constant flow of energy from the capacitors to the output load is made possible by this transition. The following are the appropriate inductor voltages, capacitor currents, and output voltage equations obtained by applying KVL and KCL:

$$V_{L_1}(t) = L_1 \frac{di_{L_1}(t)}{dt} = V_s(t) - V_{C_1}(t) \quad 3.37$$

$$V_{L_2}(t) = L_2 \frac{di_{L_2}(t)}{dt} = V_{C_1}(t) - V_{C_2}(t) \quad 3.38$$

$$i_{C_1}(t) = C_1 \frac{dV_{C_1}(t)}{dt} = i_{L_1}(t) - i_{L_2}(t) \quad 3.39$$

$$i_{C_2}(t) = C_2 \frac{dV_{C_2}(t)}{dt} = i_{L_2}(t) - \frac{V_{C_2}(t)}{R_o} \quad 3.40$$

$$V_O(t) = V_{C_2}(t) \quad 3.41$$

Equations eq. (3.37)-eq. (3.41) can be written in state space model as:

$$\begin{bmatrix} \frac{di_{L_1}}{dt} \\ \frac{di_{L_2}}{dt} \\ \frac{dV_{C_1}}{dt} \\ \frac{dV_{C_2}}{dt} \end{bmatrix} = A_2 \begin{bmatrix} i_{L_1} \\ i_{L_2} \\ V_{C_1} \\ V_{C_2} \end{bmatrix} + B_2[V_s] \qquad 3.42$$

$$[V_o] = E_2 \begin{bmatrix} i_{L_1} \\ i_{L_2} \\ V_{C_1} \\ V_{C_2} \end{bmatrix} + F_2[V_s] \qquad 3.43$$

Where,

$$A_2 = \begin{bmatrix} 0 & 0 & -\frac{1}{L_1} & 0 \\ 0 & 0 & 0 & -\frac{1}{L_2} \\ \frac{1}{C_1} & 0 & 0 & 0 \\ 0 & 1 & 0 & \frac{-1}{R_o C_2} \end{bmatrix}, B_2 = \begin{bmatrix} \frac{1}{L_1} \\ 0 \\ 0 \\ 0 \end{bmatrix} \qquad 4.44$$

$$E_2 = [0 \quad 0 \quad 0 \quad 1], F_2 = [0]$$

Step 2: State Space Averaging Equations.

According to the discussed, the large-signal non-linear averaged state-space model of QBC can be given as:

$$\begin{bmatrix} \frac{d\bar{\imath}_{L_1}}{dt} \\ \frac{d\bar{\imath}_{L_2}}{dt} \\ \frac{d\bar{V}_{C_1}}{dt} \\ \frac{d\bar{V}_{C_2}}{dt} \end{bmatrix} = \bar{A} \begin{bmatrix} \bar{\imath}_{L_1} \\ \bar{\imath}_{L_2} \\ \bar{V}_{C_1} \\ \bar{V}_{C_2} \end{bmatrix} + \bar{B}[\bar{V}_s] \qquad 3.45$$

$$[\bar{V}_o] = \bar{E} \begin{bmatrix} i_{L_1} \\ i_{L_2} \\ V_{C_1} \\ V_{C_2} \end{bmatrix} + \bar{F}[\bar{V}_s] \qquad 3.46$$

Where

$$\bar{A} = A_1 * D + A_2 * (1 - D), \bar{B} = B_1 * D + B_2 * (1 - D) \qquad 3.47$$

$$\bar{E} = E_1 * D + E_2 * (1 - D), \bar{F} = F_1 * d + F_2 * (1 - D)$$

Step 3: Perturbation and Linearization of averaged state space model.

In this context, we add minor deviations to specific variables in relation to their standard, constant (DC) values. These modifications are implemented to analyze the system's behaviour in proximity to its equilibrium or steady-state condition.

$$\bar{\imath}_{L_1}(t) = I_{L_1} + \hat{\imath}_{L_1}(t), \bar{\imath}_{L_2}(t) = I_{L_2} + \hat{\imath}_{L_2}(t)$$
$$\bar{V}_s(t) = V_s + \hat{v}_s(t), d(t) = D + \hat{d}(t) \qquad 3.48$$
$$\bar{V}_{C_1}(t) = V_{C_1} + \hat{v}_{C_1}(t), \bar{V}_{C_2}(t) = V_{C_2} + \hat{v}_{C_2}(t), \bar{V}_o(t) = V_o + \hat{v}_o(t)$$

By introducing this perturbation, and ignoring the higher order ac terms we can obtain the small signal ac model of QBC which will be given by:

$$\begin{bmatrix} \frac{d\hat{\imath}_{L_1}}{dt} \\ \frac{d\hat{\imath}_{L_2}}{dt} \\ \frac{d\hat{V}_{C_1}}{dt} \\ \frac{d\hat{V}_{C_2}}{dt} \end{bmatrix} = A \begin{bmatrix} \hat{\imath}_{L_1} \\ \hat{\imath}_{L_2} \\ \hat{V}_{C_1} \\ \hat{V}_{C_2} \end{bmatrix} + B[\hat{V}_s] \qquad 3.49$$

$$[\hat{V}_o] = E \begin{bmatrix} \hat{\imath}_{L_1} \\ \hat{\imath}_{L_2} \\ \hat{V}_{C_1} \\ \hat{V}_{C_2} \end{bmatrix} + F[\hat{V}_s] \qquad 3.50$$

Step 4: Derivation of T/F:

Now, by taking the Laplace transform and using eq. (3.25) and eq. (3.28), We can calculate various transfer function.

I. Input to Output voltage T/F:

The transfer function of input voltage to output voltage in a Quadratic Boost converter delineates the output voltage's reaction to fluctuations in the input voltage.

$$\frac{\hat{v}_o(s)}{\hat{v}_s(s)} = G_{vg}(s) = C(sI - A)^{-1}[B]_{first\ coloumn} \qquad 3.51$$

$$G_{vg}(s) = \frac{\frac{DD'}{L_1L_2C_1C_2}}{s^4 + \frac{1}{RC_2}s^3 + \left(\frac{D'^2}{L_1C_1} + \frac{D^2}{L_2C_1} + \frac{1}{L_2C_2}\right)s^2 + \frac{D^2L_1 + D'^2L_2}{RL_1L_2C_1C_2}s + \frac{D'^2}{L_1L_2C_1C_2}} \qquad 3.52$$

II. Load Current to o/p voltage T/F:

The Quadratic Boost converter's load current to output voltage transfer function shows how the voltage sent to the load changes as the load's current level changes. This shows that the converter can regulate the output voltage. This function is important for testing how the converter works with different loads to make sure it can keep the output voltage stable even when the load current changes. Developing a better understanding of this connection will lead to improvements in the design of your converter, making it work much better and more reliably in practical applications.

III. Control to O/P T/F:

The function called "duty cycle" allows the Quadratic Boost converter to demonstrate how changes in duty cycle will affect the output voltage through an o/p Voltage Transfer Function; this function is important in controlling and adjusting the output voltage so that it meets the needs of the load connected to it. This makes sure that power is delivered efficiently in a wide range of working conditions.

$$\frac{\hat{v}_o(s)}{\hat{d}(s)} = G_{vd}(s) = C(sI - A)^{-1}[(A_1 - A_2)X + (B_1 - B_2)U] \qquad 3.55$$

$$G_{vd}(s) = \frac{-\frac{1}{L_1L_2C_1C_2}\left(L_1C_1V_{C_1}s^2 - L_1I_{L_1}s + D'V_{C_1}\right)}{s^4 + \frac{1}{RC_2}s^3 + \left(\frac{D'^2}{L_1C_1} + \frac{D^2}{L_2C_1} + \frac{1}{L_2C_2}\right)s^2 + \frac{D^2L_1 + D'^2L_2}{RL_1L_2C_1C_2}s + \frac{D'^2}{L_1L_2C_1C_2}} \qquad 3.56$$

3.5 Bode Plot of Input to output voltage Transfer function

The frequency response of the quadratic boost converter is depicted in the Bode plot. The magnitude response is constant in low frequencies and decreases in high frequencies, which helps to reduce unwanted noise and switching harmonics. The phase response is frequency dependent and varies smoothly, indicating smooth dynamic performance.

This system is stable because the gain crossover occurs before phase reaches −180°. This results in positive phase margin and guarantees stable operation of the converter. Therefore, the quadratic boost converter has good stability and is suitable for photovoltaic applications.

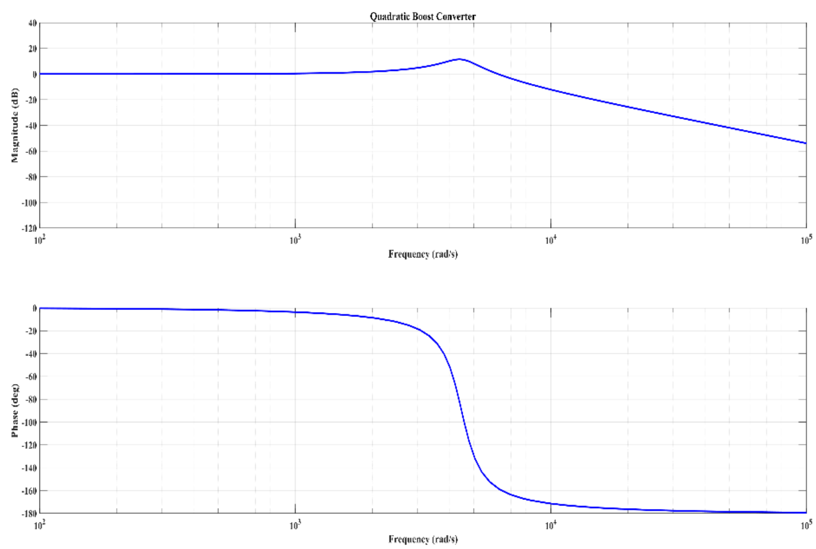

Fig.3.3 Bode Plot Of $\frac{\widehat{V_0}}{\widehat{V_s}}$

CHAPTER 4

PHOTOVOLTAIC SYSTEM INTEGRATION WITH QUADRATIC BOOST CONVERTER

4.1 INTRODUCTION

Fossil fuels continue to play a key role in producing electricity around the world, leading to significant amounts of carbon dioxide (CO_2) emissions and global climate change. To help address these issues, there has been a growing emphasis on sourcing electricity from renewable energy sources, such as solar, wind, and ocean energy systems [11]. Solar energy, in particular, is regarded as one of the most important renewable energy sources due to its availability, low impact on the environment, and ongoing development of photovoltaic (PV) technology. PV Modules, which use direct conversion of solar energy into electrical energy, continue to be one of the most promising new renewable energy technologies [12]. Despite the many benefits of PV systems, operating limits associated with environmental conditions and operational conditions can adversely affect the performance of PV modules. Temperature fluctuations, variations in solar irradiance, partial shading, dirt accumulation, and the aging of components can all result in significantly reduced output power from PV modules, due to the inability of PV cells to operate consistently in mismatched conditions (MC) [13]. To prevent shaded PV cells from overheating or developing a hotspot, bypass diodes are typically installed in parallel to PV sub-modules. While bypass diodes do offer increased safety and reliability to the PV system, they can also cause the power-voltage (P-V) characteristics of a PV array to produce multiple peaks when a PV array is partially shaded [4]. In order to carry out maximum power-point tracking, it’s important to identify the true Global Maximum Power Point (GMPP). When an array of solar panels experiences shade or other environmental inconsistencies, tracking the GMPP becomes very difficult due to multiple peak outputs from the solar array. Under uniform environmental conditions, traditional maximum power point tracking (MPPT) methods (like Perturb and Observe [P&O] and Incremental Conductance [INC]) are commonly used for their simplicity of implementation, low computational complexity, and relative speed of convergence [15], [16]. Furthermore, since these methods do not require in-depth knowledge of the parameters associated with the photovoltaic (PV) modules, their use can be justified for plug-and-play applications. On the other hand, conventional techniques may become trapped at local maximums and/or oscillate continuously at steady-state conditions around the operating point, thus creating a loss of power while decreasing efficient performance under mismatch conditions [7].

A number of advanced techniques have been proposed to enhance MPPT performance during partial shading or where non-uniformity exists. Artificial Intelligence (AI) based maximum power point tracking techniques (e.g. fuzzy logic, neural networks, and optimization algorithms) have proven that they are capable of tracking the GMPP even when dealing with complex operating conditions [8]–[10]. However, AI-based processes still often need large amounts of training data, a lot of tuning parameters, and knowledge base information about the system. Also, with rapid changing environmental conditions,many AI-based processes are still not able to accurately determine the global maximum point [11], [12].

4.2 PHOTOVOLTAIC CELL MODELLING

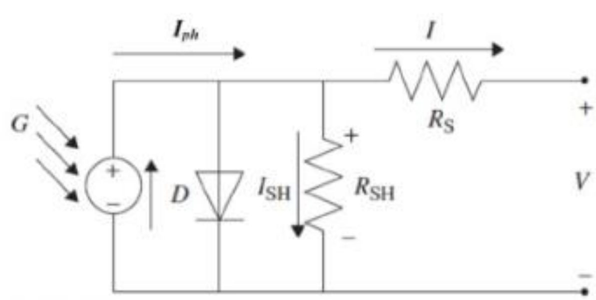

Fig.4.1: Equivalent circuit of Single Diode PV-Cell.

A PV cell is a semiconductor device that produces electricity when exposed to sunlight; this cold electricity comes from the photovoltaic effect. In reality, the equivalent circuit of a PV cell includes a current generator in parallel to a diode plus series resistance and a shunt resistance which account for all the actual losses that will be created when this device operates [10]-[12].

The mathematical equation of the PV cell output current is expressed as:

$$I = Iph - Io\,(e^{\frac{V+IRs}{nVt}} - 1) - \frac{V+IRs}{Rsh}$$

Where:
Iph = Photo-generated current

Io = Diode reverse saturation current

Rs = Series resistance

Rsh = Shunt resistance

n = Ideality factor

Vt = thermal voltage

The output characteristics of the PV panel are nonlinear and strongly influenced by irradiation and temperature variations. As solar irradiation increases, the output current and power increase, whereas an increase in temperature mainly reduces the output voltage [13]-[15].

4.3 Characteristics of PV Module

The photovoltaic module exhibits nonlinear current-voltage (I-V) and power-voltage (P-V) characteristics. These characteristics are important for understanding the operating behaviour of PV systems.

4.3.1 I–V Characteristics

The I–V curve of the PV module shows the relationship between output current and output voltage. Initially, the current remains almost constant with increasing voltage, but after a certain point, the current decreases rapidly until it reaches zero at open-circuit voltage [16].

4.3.2 P–V Characteristics

The P–V characteristic curve contains a unique operating point called the Maximum Power Point (MPP), where the PV panel delivers maximum power output [17].

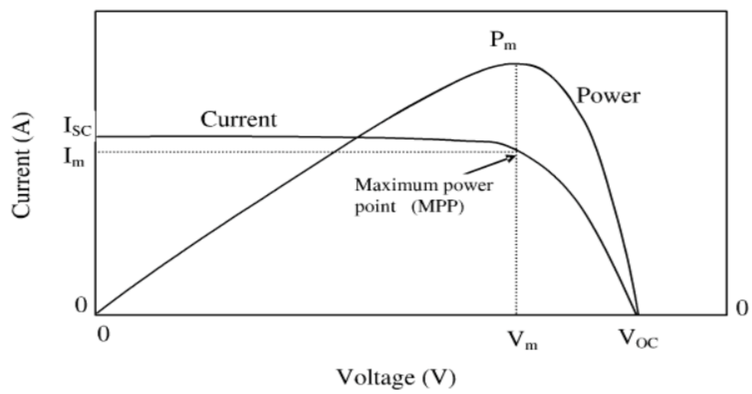

Fig.4.2: I–V and PV Characteristics

The output power of the PV module is given by:
$P=VI$

Where:

- P = Output power
- V = Output voltage
- I = Output current

The location of the maximum power point changes continuously with variations in irradiation and temperature. Therefore, an MPPT algorithm is necessary to ensure maximum power extraction from the PV system [18].

4.4 Maximum Power Point Tracking (MPPT)

Maximum Power Point Tracking (MPPT) is an essential control technique used in photovoltaic systems to maximize power extraction under varying environmental conditions [19]. Since the operating point of the PV panel changes continuously due to irradiation and temperature variations, the MPPT controller adjusts the duty cycle of the converter to operate the PV module at its maximum power point.

Among various MPPT techniques, the Perturb and Observe (P&O) algorithm is commonly used because of its simple implementation and low computational complexity [20]-[22].

The basic operating principle of the P&O algorithm is as follows:

1. Measure PV voltage and current
2. Calculate PV output power
3. Compare present power with previous power
4. Adjust duty cycle accordingly
5. Repeat the process continuously

If the power increases after perturbation, the perturbation direction remains unchanged. Otherwise, the perturbation direction is reversed. The MPPT controller generates PWM pulses to control the MOSFET switch of the Quadratic Boost Converter [23].

4.5 Integration of PV System with Quadratic Boost Converter

The proposed system integrates a photovoltaic source with a Quadratic Boost Converter to achieve high voltage gain and efficient power transfer. The PV panel provides low DC voltage, which is boosted to the required higher output voltage using the converter.

The overall system consists of:

- Photovoltaic module
- MPPT controller
- PWM generation circuit
- Quadratic Boost Converter
- Resistive load

A Maximum Power Point Tracking controller always keeps an eye on how much electricity is coming from the solar panels and adapts the converter's pulse width to keep the solar panels working at their maximum power output level.

The amount of voltage "boost" that can be provided by a quadratic boost converter operating in a continuous conduction mode is given to be:

$$\frac{V_o}{V_s} = \frac{1}{(1-D)^2}$$

Where:

- Vo = Output voltage
- Vs = Input voltage
- D = Duty cycle

Due to features of the circuit, the voltage gain that is available from a quadratic boost converter can be much higher than traditional boost converters as well as providing lower switching voltage and improved efficiency [24]–[26].

CHAPTER 5

MPPT TECHNIQUES OVERVIEW

5.1 Perturb and Observe (P&O) Technique

The Perturb and Observe (P&O) algorithm is one of the most used Maximum Power Point Tracking (MPPT) methods for PV systems, as it is relatively easy to implement and simplistic in terms of structure. The main goal of the P&O methodology is to obtain maximum power from the PV module with changing environmental conditions (i.e. temperature and irradiance), and therefore [13].

To implement the P&O method of maximum power point tracking (MPPT) for photovoltaic systems, the operation of the devices are regularly varied by changing the converter voltage or duty cycle. When a small voltage change increases the resultant output power, the perturbation applies in the same direction to continue to increase power. Conversely, if the output power decreases when the voltage changes, the perturbation will be reversed. This process is done repetitively to move to the MPP of the PV system gradually.

The P&O MPPT methodology is often used in practical implementations because it has a minimal number of sensors and has a simple algorithm, with less computational complexity than more sophisticated MPPT techniques. Additionally, the algorithm can easily be used within digital controlled devices such as microcontrollers and/or DSP-based systems. On the other hand, there are some limitations to the P&O method. While operating under steady-state conditions, the device's operating point will oscillate around the MPP of the PV system, which may cause the PV system to lose power. Additionally, the P&O algorithm may incorrectly identify the direction of the operating point when atmospheric conditions change rapidly, resulting in lower tracking accuracy and performance.

These constraints notwithstanding, the P&O technique continues to be one of the most widely used MPPT methods for photovoltaic energy conversion system applications because of its dependable performance, uncomplicated operation, and low-cost solution for implementation purposes. As a result, it is highly adopted by PV systems that use various types of DC–DC converters, such as boost converter and quadratic boost converter topologies [13].

Therefore, studying partial shade conditions has become increasingly important when designing and controlling photovoltaic energy systems. By properly modelling shading environments and applying appropriate MPPT methods, it is possible to increase the reliability of the system, improve power output from these systems, and enhance the overall efficiency of photovoltaic power conversion systems [14][15].

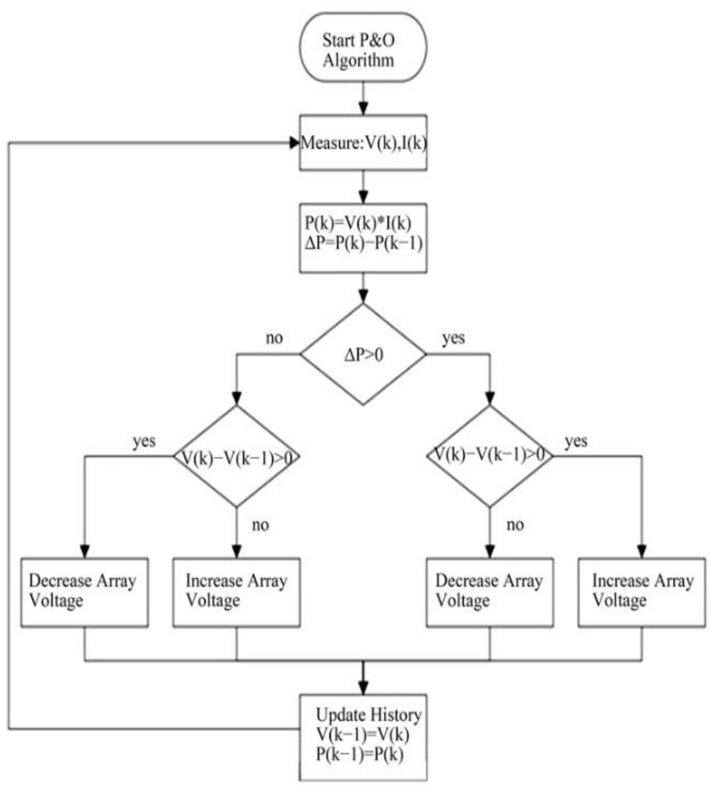

Fig.5.1: Flow Chart of P & O Technique

5.2 Incremental Conductance (INC) Technique

The Incremental Conductance (INC) technique is one of the most commonly used Maximum Power Point Tracking (MPPT) methods for photovoltaic (PV) systems. In this method, the incremental conductance (dI/dV) and instantaneous conductance (I/V) of the PV array are compared to track the maximum power point. At this maximum power point, the following equation must hold

$$\frac{dI}{dV} = -\frac{I}{V}$$

Using this principle to guide the converter's duty cycle will allow the controller to adjust the converter's output as the PV module is exposed to changing irradiance or temperature levels in order to pull maximum power from the module. By comparison to the Perturb and Observe (P&O) technique, the INC technique has demonstrated superior accuracy and reduced oscillation in MPPT performance. The INC method also works efficiently when weather conditions are changing rapidly. Unfortunately, the calculations associated with using the INC technique are much more complex than those of the P&O method. Furthermore, this method requires additional sensing devices [16], [17] to support the installation and operation of the INC technique.

CHAPTER 6

SIMULATION RESULT

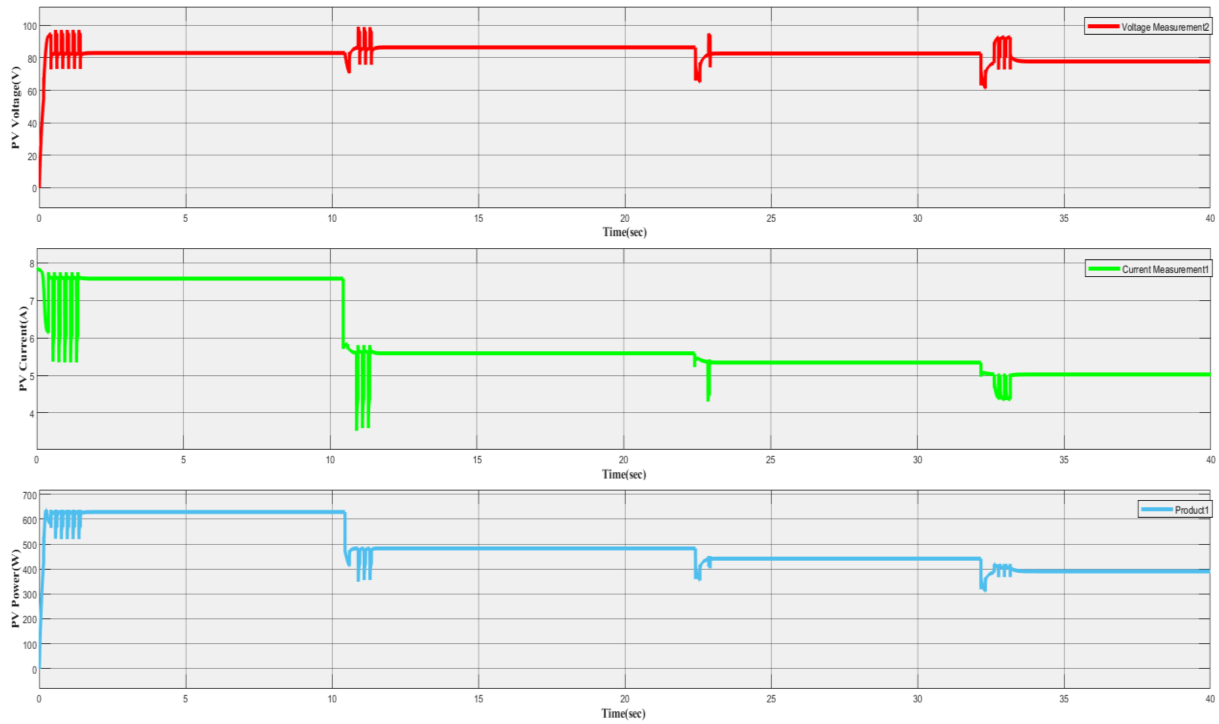

Fig.6.1: Waveform of o/p Voltage (Vpv in Volt), o/p Current (Ipv in Amp), and o/p Power (Ppv in Watt) of PV at variable Irradiance

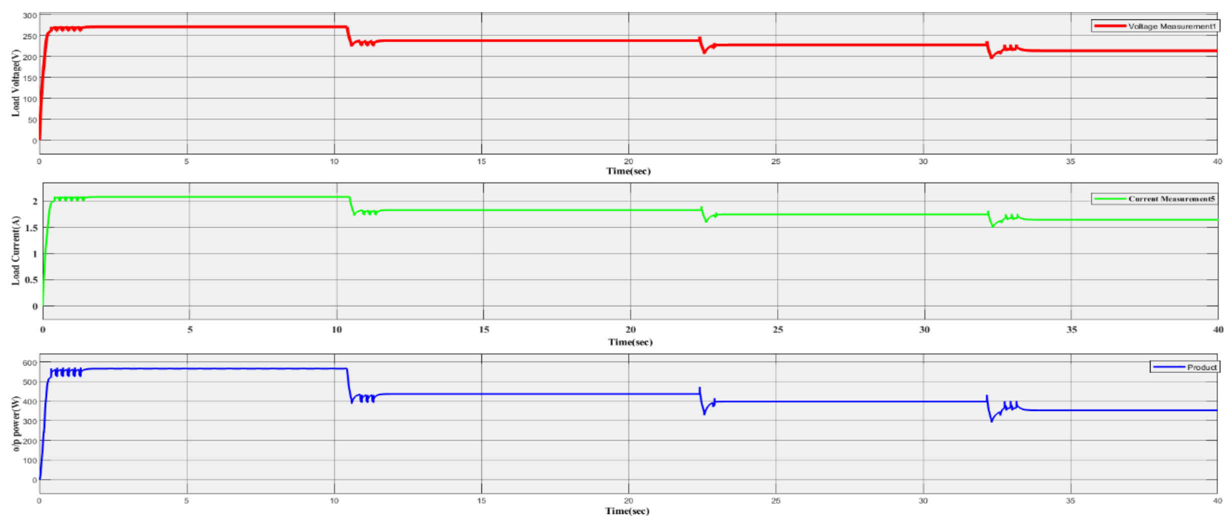

Fig.6.2: Waveform of o/p Voltage (Vo in Volt), o/p Current (Vo in Amp), and o/p Power(Po in Watt) of QBC at Variable Irradiance.

6.1 Result And Discussion

The photovoltaic system that uses Quantum Boost Converter has been tested using computer simulations done with MATLAB and Simulink software. These tests were done with amounts of sunlight including 1000 W/m^2, 850 W/m^2, 750 W/m^2 and 650 W/m^2. The goal of these tests was to see how the photovoltaic system works, how well the Maximum Power Point Tracking method performs and how well the converter amplifies voltage in conditions.

Figure 8.1 shows how the voltage, current and power of the photovoltaic system change with amounts of sunlight. The results of the tests show that the photovoltaic system produces the power when it gets 1000 W/m^2 of sunlight. When the sunlight is reduced from 1000 W/m^2 to 650 W/m^2, the current and power produced by the photovoltaic system decrease significantly. The voltage of the photovoltaic system stays the same throughout the test. This is what we expect from photovoltaic systems because the amount of sunlight mainly affects the current produced by the photovoltaic system. The photovoltaic system works this way because the photovoltaic system is sensitive, to sunlight.

The designed Perturb and Observe (P&O)-based MPPT algorithm automatically modifies the converter duty cycle to keep the operation of the system close to the maximum power point. It can be seen from the results that the controller tracks the maximum power available at any level of irradiance. The operation of the tracking remains stable during the change of irradiance levels and allows efficient exploitation of available solar energy.

Figure 8.2 shows the voltage, current, and power at the output of the Quadratic Boost Converter. This converter manages to amplify low-voltage output power generated by the PV panel. Despite changes in the level of solar irradiance, satisfactory voltage regulation and stable operation of the converter is achieved throughout the whole process of testing.

In case the solar irradiance is at its highest level, i.e., 1000 W/m^2, maximum output power is provided due to the high energy input received by the solar panel. At reduced irradiance levels of 850 W/m², 750 W/m², and 650 W/m², there is a gradual decrease in both output current and power. Output voltage still stays within the required range for the Quadratic Boost Converter.

The simulation findings further indicate that the converter performs at reduced voltage ripple and good current behaviour. The energy transfer between the source and the load continues to be effective throughout the whole range of irradiance values in consideration in this project. The combination of both the MPPT controller and Quadratic Boost Converter ensures optimal power transfer and efficiency.

From all the results above, it is evident that the suggested Quadratic Boost Converter fed by photovoltaic works well, giving steady output voltage with high voltage gain and good power transfer efficiency despite changing irradiance levels. The performance parameters discussed above make this proposed system a suitable choice for renewable energy applications including photovoltaic systems, battery chargers, and DC microgrids among others.

6.2 Summary

- Power obtained is maximized when there is 1000 W/m² irradiance.
- PV current falls directly as irradiance decreases.
- The perturbation and observation technique accurately follows the maximum power point.
- Voltage gain is very high using the Quadratic Boost Converter.
- The output voltage is well regulated regardless of irradiance variations.
- There is low ripple within the converter throughout the entire process.
- The combination of the PV and QBC system performs effectively.

CHAPTER 7

CONCLUSION AND FUTURE SCOPE

10.1 Conclusion

We designed and constructed a Quadratic Boost Converter that uses a PV source for applications requiring a high gain (DC-DC). The converter was modelled using the state-space averaging method and integrated into the PV system, which is being used to generate renewable energy. A Maximum Power Point Tracking (or MPPT) algorithm based on Perturb and Observe (P&O) was developed to maximize available energy from the PV panel as atmospheric conditions change.

The PV system was modelled to simulate different irradiation and temperature conditions. The PV integrated Quadratic Boost Converter has been modelled and analyzed in MATLAB/Simulink. The results of the simulations showed stable converter operation, fast dynamic response, increased voltage conversion ratio, and efficient transfer of energy from the PV system to the load. The converter functioned well, increasing the low voltage of the PV system into a higher desired output voltage while producing low ripple and having good efficiency. MPPT continuously adjusted the converter's duty cycle to ensure operation at maximum power point.

In addition to designing the PCB and hardware for implementation of a practical realization of the system, many of the renewable energy applications include such things as battery storage systems, electric vehicle charging systems, stand-alone solar systems, and DC 'micro-grids.' Overall, the PV integrated Quadratic Boost Converter provides an effective solution.

7.2 Future Scope

1. Fuzzy and Neural Networks are more advanced MPPT algorithms allowing for improved performance of tracking.

2. Using Closed Loop Controllers (PID and Sliding Mode) provides better regulation of voltage.

3. Testing of a hardware prototype can also take place in actual environmental conditions.

4. The converter can be adapted for use with Electric Vehicle (EV) Chargers and Grid Connect Solar Systems.

5. Integration of IOT-based monitoring and intelligent control will allow for the development of smart renewable energy applications.

REFERENCES

[1].M. H. Rashid, Power Electronics Handbook, 2nd ed. Academic Press, 2001.
[2].R. W. Erickson and D. Maksimovic, Fundamentals of Power Electronics, 2nd ed. Kluwer Academic Publishers, 2001
[3].B. K. Bose, "Evaluation of modern power semiconductor devices and future trends of converters," IEEE Trans. Ind. Appl., vol. 28, no. 2, pp.403–413, 1992.
[4].S. Gopinathan, V. S. Rao, and K. Sundaramoorthy, "Family of non-isolated quadratic high gain DC–DC converters based on extended capacitor-diode network for renewable energy source integration," IEEE J. Emerg. Sel. Topics Power Electron., vol. 10, no. 5, pp. 6218–6230, Oct. 2022.
[5].P. Imbertson and N. Mohan, "A method for estimating switch-mode power supply size," in Proceedings, Fourth Annual IEEE Applied Power Electronics Conference and Exposition, 1989.
[6].M. Veerachary, "Design and analysis of a new quadratic boost converter," in *2017 National Power Electronics Conference (NPEC)*, Pune, India, 2017, pp. 307–313, doi:10.1109/NPEC.2017.8310476.
[7].A. Balal and F. Shahabi, "LTspice Analysis of Double-Inductor Quadratic Boost Converter in Comparison with Quadratic Boost and Double Cascaded Boost Converter," in *2021 12th International Conference on Computing Communication and Networking Technologies (ICCCNT)*, Kharagpur, India, 2021, pp. 1–6, doi:10.1109/ICCCNT51525.2021.9579931.
[8].N. Mohan, T. M. Undeland, and W. P. Robbins, *Power Electronics: Converters, Applications, and Design*, 3rd ed. Hoboken, NJ, USA: John Wiley & Sons, 2003.
[9].R. W. Erickson and D. Maksimović, *Fundamentals of Power Electronics*, 2nd ed. New York, NY, USA: Springer, 2001.

[11]. M. Forouzesh, Y. P. Siwakoti, S. A. Gorji, F. Blaabjerg, and B. Lehman, "Step-up DC–DC converters: A comprehensive review of voltage-boosting techniques, topologies, and applications," *IEEE Transactions on Power Electronics*, vol. 32, no. 12, pp. 9143–9178, Dec. 2017.

[12].N. Altin and E. Ozturk, "Maximum power point tracking quadratic boost converter for photovoltaic systems," in *2016 8th International Conference on Electronics, Computers and Artificial Intelligence (ECAI)*, Ploiesti, Romania, 2016, pp. 1–4, doi:10.1109/ECAI.2016.7861151.

[13].D. Anusha, S. Youvaraj, G. Youvaraj, H. Bhanarkar, B. Marupatla, and S. Pradabane, “A Single Switch Structured Improved Quadratic Boost Converter for Renewable Energy Applications,” in *2025 International Conference on Power Electronics Converters for Transportation and Energy Applications (PECTEA)*, Jatni, India, 2025, pp. 1–5, doi:10.1109/PECTEA61788.2025.11076381.

[14].G. Mutezo, J. Mulopo, A review of Africa’s transition from fossil fuels to renewable energy using circular economy principles, Renew. Sustain. Energy Rev. 137 (2021) 110609, http://dx.doi.org/10.1016/j.rser.2020.110609.

[15].R.G. Mohamed, H.M. Hasanien, M. Ebrahim, Global MPPT controllers for enhancing dynamic performance of photovoltaic systems under partial shading condition, E-Prime-Adv. Electr. Eng. Electron. Energy 9 (2024) 100638, http: //dx.doi.org/10.1016/j.prime.2024.100638.

[16].M. Dhimish, Assessing MPPT techniques on hot-spotted and partially shaded photovoltaic modules: Comprehensive review based on experimental data, IEEE Trans. Electron Devices 66 (3) (2019) 1132–1144, http://dx.doi.org/10.1109/ TED.2019.2894009.

[17].M. Nusrat, S. Mekhilef, M. Mubin, S. Ahmed, M. Seyedmahmoudian, A. Stojcevski, O. Alshammari, Advancements in flexible power point tracking and power control strategies for photovoltaic power plants: A comprehensive review, Energy Rep. 12 (2024) 237–250, http://dx.doi.org/10.1016/j.egyr.2024.06.012.

[18].S. Bhattacharyya, D.S. Kumar P, S. Samanta, S. Mishra, Steady output and fast tracking MPPT (SOFT-MPPT) for P&O and InC algorithms, IEEE Trans. Sustain. Energy 12 (1) (2021) 293–302, http://dx.doi.org/10.1109/TSTE.2020.2991768.

[19].R.I. Jabbar, S. Mekhilef, M. Mubin, K.K. Mohammed, A modified perturb and observe MPPT for a fast and accurate tracking of MPP under varying weather conditions, IEEE Access 11 (2023) 76166–76176, http://dx.doi.org/10.1109/ ACCESS.2023.3297445.

[20]’S.-P. Ye, Y.-H. Liu, H.-Y. Pai, A. Sangwongwanich, F. Blaabjerg, A novel ANNbased GMPPT method for PV systems under complex partial shading conditions, IEEE Trans. Sustain. Energy 15 (1) (2024) 328–338, http://dx.doi.org/10.1109/ TSTE.2023.3284866.

[21].T. Hai, A.K. Alazzawi, J. Zhou, H. Farajian, Performance improvement of PEM fuel cell power system using fuzzy logic controller-based MPPT technique to extract the maximum power under various conditions, Int. J. Hydrog. Energy 48 (11) (2023) 4430–4445, http://dx.doi.org/10.1016/j.ijhydene.2022.10.103. 12 I.J. Pal and V.V. Ramana Renewable Energy 259 (2026) 125047.

[22].A. Hassan, O. Bass, M.A. Masoum, An improved genetic algorithm based fractional open circuit voltage MPPT for solar PV systems, Energy Rep. 9 (2023) 1535–1548, http://dx.doi.org/10.1016/j.egyr.2022.12.088.

[23].T.H. Pham, B. Raahemi, Bio-inspired feature selection algorithms with their applications: a systematic literature review, IEEE Access 11 (2023),43733–43758, http://dx.doi.org/10.1109/ACCESS.2023.3272556.

[24].A. Singh, V. Siva, A. Kumar, and S. K. Singh, "Analysis and design of switched LC converter with reduced voltage stress for photovoltaic applications," *IEEE Trans. Ind. Appl.*, vol. 59, no. 5, pp. 6468–6479, Sep./Oct. 2023.

[25].P. K. Pardhi and S. K. Sharma, "High gain non isolated DC converter employed in single-phase grid-tied solar photovoltaic supply system," IEEE Trans. Ind. Appl., vol. 57, no. 5, pp. 5170–5182, Sep./Oct. 2021.

[26].S. Gopinathan, V. S. Rao, and K. Sundaramoorthy, "Family of non-isolated quadratic high gain DC–DC converters based on extended capacitor-diode network for renewable energy source integration," IEEE J. Emerg. Sel. Topics Power Electron., vol. 10, no. 5, pp. 6218–6230, Oct. 2022.

[27]. F. L. Luo and H. Ye, *Advanced DC/DC Converters*. Boca Raton, FL, USA: CRC Press, 2004.

[28]. Y. P. Siwakoti and F. Blaabjerg, "A review of magnetically coupled impedance-source DC–DC converters," *IEEE Transactions on Power Electronics*, vol. 33, no. 6, pp. 4929–4944, Jun. 2018.

.